# Heavy Metal Detection based on Coreless Fibers Using the LSPR Technique

**Mohammed S. Sada[1*], Bushra R. Mahdi[2], Hashim Ali[3], Nahla A. Aljbar[4], Mahdi A. Mohammed[5]**

## Abstract

In this study, a fiber optic sensing probes based on localized surface Plasmon resonance was presented to detect various Heavy metal zinc concentrations in an aqueous solution. The fiber optic sensing probe consists of a single mode fiber-coreless fiber-single mode fiber structure coated with a 40 nm thickness of gold nanoparticles - polyvinyl pyrrolidone using an immersion method. The results obtained in the experiment showed that the sensor's sensitivity is 1.38 nm/ppm in the range of 0 to 6 ppm concentrations.

**Key Words:** Fiber Optic, Coreless Fiber, Sensing Probes, Heavy Metal.

**DOI Number: 10.14704/nq.2021.19.7.NQ21087** **NeuroQuantology 2021; 19(7):78-83**

## Introduction

As a result of the great industrial development, drinking water is exposed to pollution, making it unsuitable for drinking. Among the most prominent water pollutants are toxic heavy metals (such Zn), so their detection is extremely important. There are various detection methods such as atomic absorption method (Jarzyńska et al, 2011), spectrophotometry method (Pehlivan et al, 2009), inductively coupled plasma mass spectrometry method (Chen *et al*, 2013), chemiluminescence method (Tsukagoshi *et al*, 2000), and electrochemical approaches method (Bakhtiarzadeh et al, 2008). Though sensitive, but very tedious, these methods are expensive and involve huge tools to operate. A simple, sensitive, easy, inexpensive and straightforward analysis method is required. One option for this is a fiber optic sensor based on (LSPR).

Researchers have developed fiber-based (LSPR) sensors on a large scale by several manufacturing methods, such as side polishing (Jing *et al*, 2019), fiber's etching (Coelho *et al*, 2015), the use of tilted fiber Bragg grating (Caucheteur *et al*, 2011)or long period fiber grating (Hu *et al*, 2014), also utilizing distinctive fiber like photonic crystal fibers (Rifat *et al*, 2018)or coreless fiber (CF) (Han *et al*, 2019). For a number of reasons, CF-based LSPR sensors stand out among these schemes, including the lack of complicated fiber pre-processing, inexpensive, simplicity of fabrication, and low insertion loss. It's perfect for environmental applications because of these benefits.



## Experimental

### *Preparation of Zn Solution with Water*

Zn solution was prepared with 1ppm concentration by dissolving a 1mg of zinc nitrate ($Zn(NO_3)_2$) in 1L of distilled water and then stirred using magnetic stirrer until dissolved. This step was repeated to prepare 2ppm, 3ppm, 4ppm, 5ppm and 6ppm zinc solution concentration.

**Corresponding author:** Mohammed S. Sada

**Address:** [1*]Department of Physics, College of Science, Wasit University, Al Kut, Iraq; [2]Directorate of Materials Research, Laser centre, Ministry of Science and Technology, Baghdad, Iraq; [3]Department of Physics, College of Science, Wasit University, Al Kut, Iraq; [4]Directorate of Materials Research, Laser Centre, Ministry of Science and Technology, Baghdad, Iraq; [5]Department of Physics, College of Science, Wasit University, Al Kut, Iraq.

[1*]E mail: msahaam624@uowasit.edu.iq; [2]boshera65m@gmail.com; [3]hashim@uowasit.edu.iq; [4]nahla2003n@gmail.com [5]mahmed@uowasit.edu.iq

**Relevant conflicts of interest/financial disclosures:** The authors declare that the research was conducted in the absence of any commercial or financial relationships that could be construed as a potential conflict of interest.

**Received:** 14 May 2021 **Accepted:** 18 June 2021

### *Synthesis of Gold Nanoparticles (Au NPs)*

In a two-electrode electrochemical cell, gold nanoparticles are synthesized using the Electrolysis process as seen in the figure 1.a. Two electrodes of 99% purity gold were made, one anode and the other as a cathode, and the two electrodes were immersed vertically face-to-face at a constant distance of 4 cm in distilled water. The electrodes (gold) are electrically connected to the electric voltage through the voltage regulator. When a voltage (30 volts) is applied, the crystal lattice of the gold metal is destroyed and then gold starts vaporizing and the vapour condense into the distilled water to form to the particles of colloidal size. Thus, we got the gold solution and tested the size of the minutes in the simplest way, which is to pass the laser through the solution. The laser beam appeared as a straight line along its path through the colloidal solution of the gold nanoparticles, as shown in Figure 1.b, which indicates that the particles are of the nanoscale size. The prepared gold nanoparticle colloidal solution is taken and dissolved in it (0.1 g) of the polymer (PVP) at a temperature of (60-70 degrees Celsius). At that time, a polymer is obtained with nanoparticles in gold (Au-NPs/PVP). After that, the solution was cooled down to room temperature while being stirred continuously. The sizes of the NPs described in this experiment are 15 and 30 nm and has been verified by transmission electronic microscopy (TEM) Figure 1.d. It can be seen for the image that particles are approximately spherical. The prepared (Au-NPs/PVP) colloid was stored at room temperature as shown in Figure 1c.

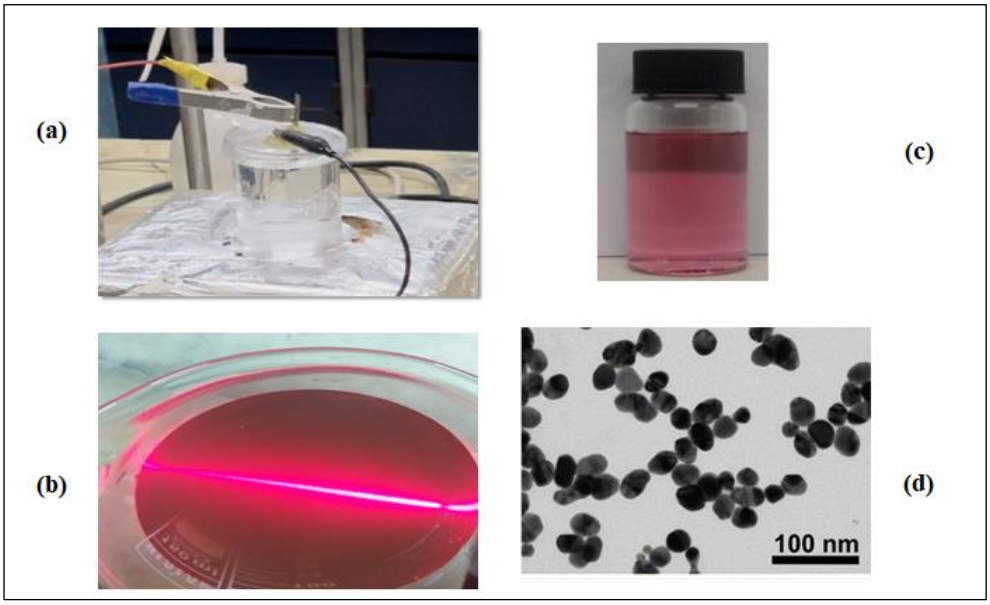


**Figure 1.** (a) photograph of Au nanoparticle synthesis in distilled water by two-electrode electrochemical cell. (b) Mechanism for testing the particle size of Au-nanoparticle. (c) Colloidal Solution. (d) TEM image of Au nanoparticle



### *Fabrication of Fiber Optic Sensing Probe*

The sensing portion includes a segment of coreless fiber (CF) (FG125LA from Thorlabs) 2.5 cm long and 125 µm as the outer diameter. The optical fiber stripper (JIC - 375 Tri - Hole) (by Fujikura Corporation) was used to remove the polymer coating from (CF), and the Fiber Cleaver (CT-30) was used to cut the part (CF) to the length required and by an angle of 90 ° to create to achieve a perfectly flat and smooth end face. Two SMF ((Corning 8/125 µm) and a CF have been fusion-spliced via commercial fiber splicer (FITEL-S178) in the manual-mode (Fujikura FSM-60S). The cladding of the sensing region was etched from 125 to 18 µm by a chemical etching process to boost the efficiency of the sensing probe and make it more sensitive to heavy metals. Finally, a gold nanoparticles - polyvinyl pyrrolidone with a 40 nm thickness has been coated on CF's surface via the use of the immersion method. Also, gold was selected since it is providing high sensitivity and good stability compared to other often utilized LSPR coating materials, like copper and silver.

### *Principle of the Mechanism of Sensing*

Light beam transmits via SMF to the CF, which has an approximate gaussian-shaped field intensity distribution which causes interference with several

directed modes that spread along the CF. Input field self images are generated at periodic intervals along with the CF due to interference between these excited modes. The output transmission spectrum's central wavelength can be expressed as follows(Alsweefe et al, 2018; Ayesh *et al*, 2016):

$$\lambda_{\mathrm{c}} = p\left(\frac{n_{\mathrm{CF}}\, d_{\mathrm{CF}}^2}{L_{\mathrm{CF}}}\right) \ldots\ldots\ldots\ldots (1)$$

Here, $p$ represents a self imaging number, $d_{CF}$ and $n_{\mathrm{CF}}$ representing the diameter and effective refractive index (RI) of the CF section, while $L$ represents CF's length. As seen in Eq (1), the diameter d CF has been proportional (inversely) to the central wavelength. With the reduction of CF's diameter, evanescent wave (EW) is formed in the gold nanoparticles - polyvinyl pyrrolidone and after that disperse to the (sensing medium). The penetration depth ($d_p$) of this evanescent wave:

$$d_p = \frac{\lambda_{\mathrm{c}}}{2\pi\, n_{\mathrm{CF}} \sqrt{\sin^2\theta - \left(\frac{n_s}{n_{\mathrm{CF}}}\right)^2}} \ldots\ldots\ldots\ldots (2)$$

Where ($n_s$) denotes the sensing medium's refractive index (RI) and ($\theta$) denotes the light's incident angle on the fiber cladding. The diameter related to the etched area as well as the sensing medium's (RI) are connected to the evanescent wave's overflow. At the core/metal interface, the propagation constant of the (EW) is given by (Gupta et al, 2018; Li, 2020):

$$\beta_{\mathrm{ev}} = \frac{2\pi}{\lambda_i}\, n_{co}\, \sin\theta \ldots\ldots\ldots\ldots (3)$$

Where $n_{co}$ is core refractive index $\lambda_i$ the wavelength of incident light and $\theta$ is the angle of the incident light at the core/metal interface. At the same time, the propagation constant ( $\beta_{\mathrm{SP}}$ ) of the surface plasm wave spreading along the interface between the medium and metal is written from Maxwell's equations(Gupta et al, 2018; Li, 2020) as follows:

$$\beta_{\mathrm{SP}} = \frac{2\pi}{\lambda_{SP}} \sqrt{\frac{\varepsilon_{\mathrm{m}} n_s^2}{\varepsilon_{\mathrm{m}} + n_s^2}} \ldots\ldots\ldots\ldots (4)$$

Where $\lambda_{SP}$ is the wavelength of the SPR, $\boldsymbol{\varepsilon_{\mathrm{m}}}$ is the dielectric constants of the metal and $\boldsymbol{n_{\mathrm{s}}}$ is the refractive index of the sensing medium. Through Equation (4), we will see that the $\beta_{\mathrm{SP}}$ at the same given wavelength $\lambda_{SP}$ is determined by that of the permittivities of a metal and also a sensing medium, i.e., $\varepsilon_{\mathrm{m}}$ and $\varepsilon_{\mathrm{s}} = n_s^2$.

SP are excited when the evanescent wave vector matches that of SPs ($\beta_{\mathrm{SP}} = \beta_{\mathrm{ev}}$) at a particular angle (resonant angle $\theta_{res}$ ), the reflected light intensity decreases to a minimum. At certain resonant wavelengths, these excited surface plasmons will produce a strong localized electromagnetic field, scattering light and forming plasmon absorption bands(Tu, Sun et al, 2012). Changes in the concentrations related to the sensing-medium will result in changes in the wave-vector of SP, and thus the excitation light's necessary wave-vector. The amplitude, phase, polarization, and spectral distribution of the excitation light determine the wave-vector of the light. As a consequence, any change in the concentrations at or near the metal-fiber interface affects these characteristics. As a result, by measuring changes in the optical parameters regarding the reflected light, the concentrations changes over the sensing surface might be identified.

## *Experimental Setup*

The experimental set-up for the zinc coreless fiber sensors is shown in Figure 2. The device is using a spectral analysis related to LSPR. Also, the experimental setup includes a laser (450 nm, 5000 mW) as a source of light, a plastic U-groove to fix the fabricated sensing probe, also to keep the fluid sample as well a spectrum analyzer (OSA) with 0.02 nm resolution as an SPR detection system. A laser source is connected to one end of the SMF, and a sensing probe (CF) is placed in a plastic U-groove that contains a test solution. The other end of the SMF has been connected to an optical spectrum analyzer for monitoring the output transmission spectrum. Also, the output transmission spectrum is monitored continuously at various Zn concentrations. Furthermore, the spectrometer has been connected to a computer through the Spectra Suite software, which is a program developed by Ocean Optics for real-time data acquisition from spectrometers. All spectra are plotted using Origin Pro 9 (Origin Lab).

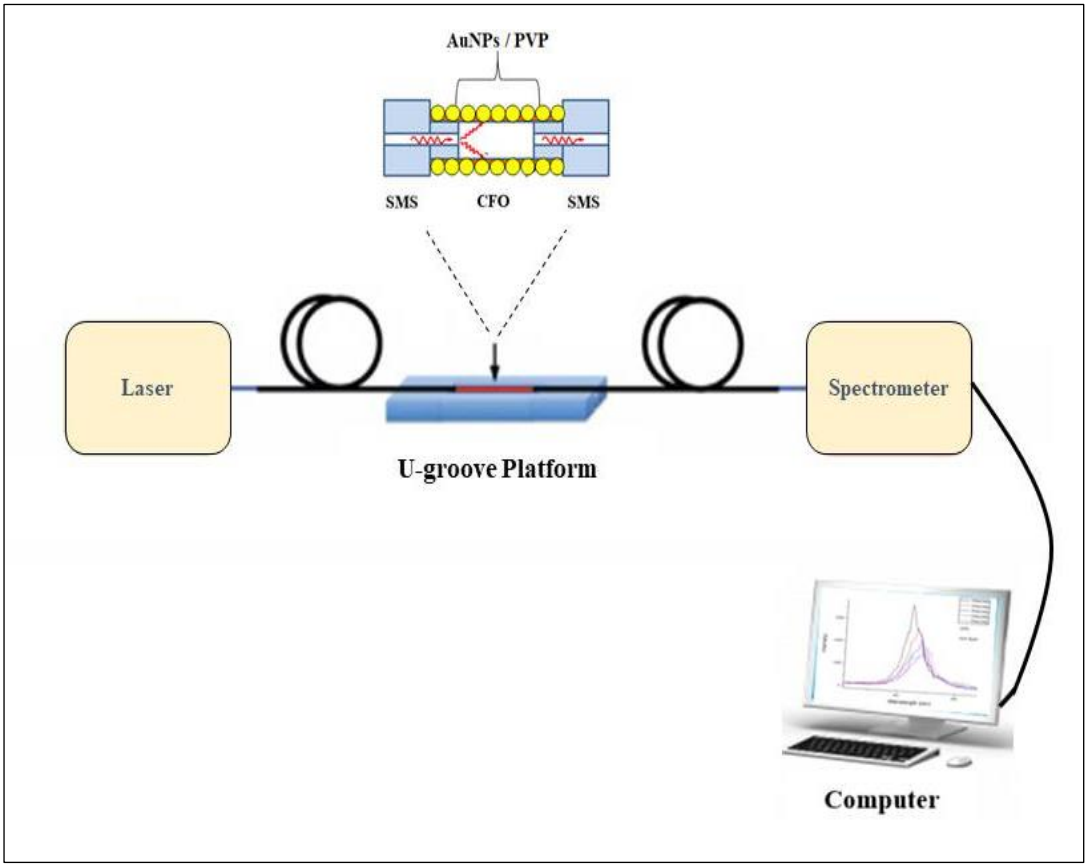


**Figure 2.** Schematic diagram of the (CFO)sensing probe



## Result and Discussion

An in-depth analysis of the sensor response to zinc (Zn) variations was performed. The sensor characterization was conducted by using fabricated sensing probe in the 0ppm to 6ppm concentration range. After each 10 minutes of stabilizing the transmission spectrum, we registered the concentration around the probe to ensure uniformity.

Figure 3. show the localized surface plasmon resonance (LSPR) spectra as a function of concentrations different of zinc (Zn) solution ranging from (0-6) ppm at room temperature for the fabricated coreless fiber (CF) sensing probe, which were illustrated in section (2.3).

The LSPR spectra of this sensing probe shows a pronounced red-shifts of the wavelength or the resonance wavelength with the increase of concentration from 0ppm to 6ppm, which confirms the LSPR phenomenon (Bao *et al*, 2019).

Because of this, as per the literature, the wavelength increases, the effective refractive index of the nearby the plasmon layer increases, it becomes increasingly important for optical designers to explore ways to use highly precise coating techniques. Here, the redshift of the wavelength with the increasing zinc (Zn) solution concentration due to of the increasing refractive index of Au NPs colloid as the concentration increases.

It may also be noted from Figure 3 that the LSPR curves broaden as the concentration of (Zn) ions increases. The broadening of LSPR curves, generally, occurs due to the increase in the number of reflections in the sensing region or due to the increase in the refractive index of the sensing medium. In the present case the number of reflections in the sensing region is fixed because same probe was used for all the LSPR curves. Thus, the only remaining reason of the broadening of the LSPR curves is the increase in the refractive index of the sensing layer due to the increase in the concentration of (Zn) ions. In other words, increase in the concentration of (Zn) ions increases its interaction with the Au NPs colloid and hence increases the refractive index of the Au NPs colloid.

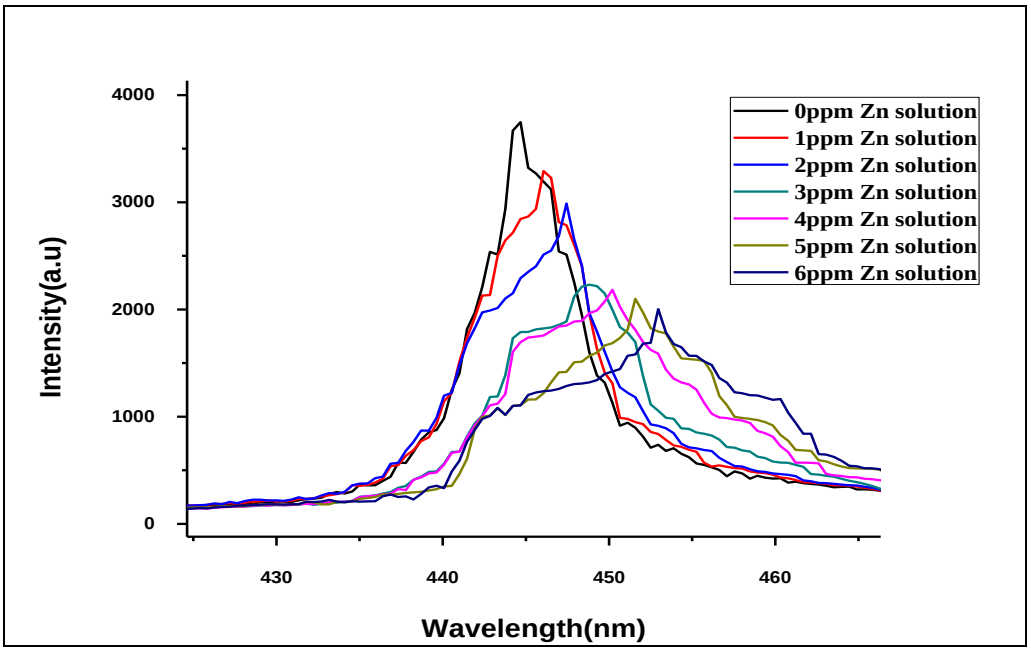


**Figure 3.** LSPR spectra response of (AuNPs–PVP)-coated coreless fiber with various Zn concentrations (0 ppm to 6ppm)

Figure 4. shows the relationship between the LSPR wavelength and concentration of zinc. It is clear from the figure that there was a good linear relationship between wavelength and concentrations. Based on the linear fitting of the data, when the concentration changes from 0ppm to 6ppm, the concentration sensitivity of this optical fiber sensors coated with a 40 nm thickness of nano-gold polymer coreless fibers is 1.38 nm/ppm.



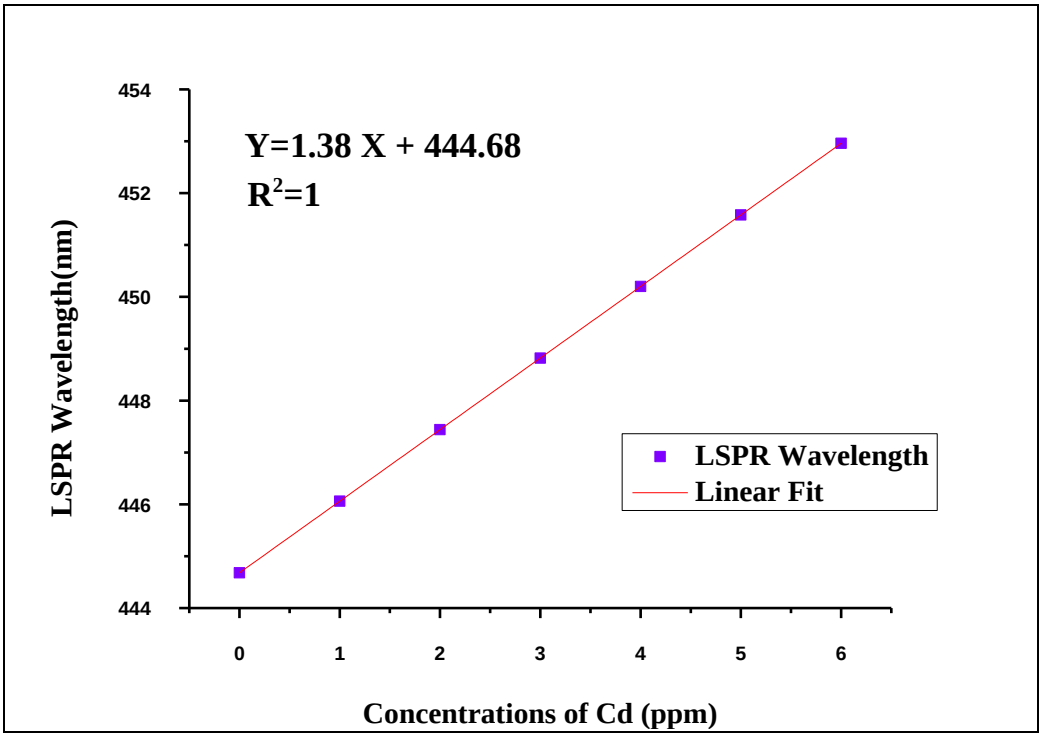


**Figure 4.** Sensitivity of the (AuNPs–PVP)-coated fiber

## Conclusion

A highly sensitive heavy metals sensor based on a sensor probe and a nano-gold polymer acting as a cladding layer has been successfully developed in this contribution. An experimental zinc sensing contrast was performed using an etched sensor

probe coated with a 40 nm thickness of nano-gold polymer. The sensor probe showed much higher sensitivity.

## Declaration of Competing Interest

The authors declare that there are no conflicts of interest.

## Acknowledgements

This work was supported by the Ministry of Science and Technology (MOSAT); Baghdad, Iraq.

## References

Alsweefe H, Al-Hayali S, Al-Janabi A. Efficient humidity sensor based on an etched no-core fiber coated with copper oxide nanoparticles. *Journal of Nanophotonics* 2018; 12(4): 46-48.

Ayesh AI, Abu-Hani AF, Mahmoud ST, Haik Y. Selective H2S sensor based on CuO nanoparticles embedded in organic membranes. *Sensors and Actuators B: Chemical* 2016; 231: 593-600.

Bakhtiarzadeh F, Ab Ghani S. An ion selective electrode for mercury (II) based on mercury (II) complex of poly (4-vinyl pyridine). *Journal of Electroanalytical Chemistry* 2008; 624 (1–2): 139–143.

Bao Y, Huang Y, Hoehler MS, Chen G. Review of fiber optic sensors for structural fire engineering. *Sensors (Switzerland)* 2019; 19(4): 1–23.

Caucheteur C, Shevchenko Y, Shao LY, Wuilpart M, Albert J. High resolution interrogation of tilted fiber grating SPR sensors from polarization properties measurement. *Optics express* 2011; 19(2): 1656–1664.

Chen X, Han C, Cheng H, Wang Y, Liu J, Xu Z, Hu L. Rapid speciation analysis of mercury in seawater and marine fish by cation exchange chromatography hyphenated with inductively coupled plasma mass spectrometry. *Journal of Chromatography a* 2013; 1314: 86-93.

Coelho L, De Almeida JMMM, Santos JL, Ferreira RAS, André PS, Viegas D. Sensing structure based on surface plasmon resonance in chemically etched single mode optical fibres. *Plasmonics* 2015; 10(2): 319-327.

Gupta D, Kant R. Recent advances in surface plasmon resonance based fiber optic chemical and biosensors utilizing bulk and nanostructures. *Optics & Laser Technology*, 2018; 101: 144–161.

Han F, Lang T, Mao B, Zhao C, Kang J, Shen C, Wang D. Surface plasmon resonance sensor based on coreless fiber for high sensitivity. *Optical Fiber Technology* 2019; 50: 172–176.

Hu HF, Deng ZQ, Zhao Y, Li J, Wang Q. Sensing properties of long period fiber grating coated by silver film. *IEEE Photonics Technology Letters* 2014; 27(1): 46–49.

Jarzyńska G, Falandysz J. The determination of mercury in mushrooms by CV-AAS and ICP-AES techniques. *Journal of Environmental Science and Health Part A* 2011; 46(6): 569–573.

Jing N, Zhou J, Li K, Wang Z, Zheng J, Xue P. Refractive index sensing based on a side-polished macrobend plastic optical fiber combining surface plasmon resonance and macrobending loss. *IEEE Sensors Journal* 2019; 19(14): 5665-5669.

Li J. A review: Development of novel fiber-optic platforms for bulk and surface refractive index sensing applications. *Sensors and Actuators Reports* 2020; 2(1): 100018.

Pehlivan E, Cetin, S. Sorption of Cr (VI) ions on two Lewatit-anion exchange resins and their quantitative determination using UV–visible spectrophotometer. *Journal of Hazardous Materials* 2009; 163(1): 448–453.

Rifat AA, Haider F, Ahmed R, Mahdiraji GA, Adikan FM, Miroshnichenko AE. Highly sensitive selectively coated photonic crystal fiber-based plasmonic sensor. *Optics letters* 2018; 43(4): 891-894.

Tsukagoshi K, Hashimoto M, Nakajima R, Arai A. Application of microchip capillary electrophoresis with chemilumine scence detection to an analysis for transition-metal ions. *Analytical sciences* 2000; 16(11): 1111-1112.

Tu M, Sun T. Optimization of gold-nanoparticle-based optical fibre surface plasmon resonance (SPR)-based sensors. *Sensors and Actuators B: Chemical* 2012; 164(1): 43–53.

Hu J, Jiang H, Liang H, Yang H. Change of cerebral structural plasticity of track athletes based on magnetic resonance imaging. *NeuroQuantology* 2018; 16(6): 758-762.